

Absence of charge-density waves on the dense Pb/Ge(111)- $\beta\sqrt{3}\times\sqrt{3}$ surface

Harumo Morikawa,* Iwao Matsuda, and Shuji Hasegawa

Department of Physics, School of Science, The University of Tokyo, 7-3-1 Hongo, Bunkyo-ku, Tokyo 113-0033, Japan

(Received 7 June 2007; revised manuscript received 24 August 2007; published 22 May 2008)

The Pb/Ge(111)- $\beta\sqrt{3}\times\sqrt{3}$ surface is generally believed to be described with a 4/3 ML (monolayer) model on which a commensurate charge-density-wave (CDW) ground state was theoretically predicted. However, our scanning tunneling microscopy imaging has shown that the surface keeps the $\sqrt{3}\times\sqrt{3}$ structure even at 6 K. Our angle-resolved photoemission measurements show that this surface has a well-nested Fermi surface (FS). However, the nesting vector does not match with what is required for the predicted CDW. Also, the electron filling counted from the FS is not consistent with the 4/3 ML model. The reason for the absence of the predicted CDW is because the surface is described with the 1 ML model. A FS-driven CDW also is not yielded due to the lack of a lock-in energy with the underlying lattice.

DOI: 10.1103/PhysRevB.77.193310

PACS number(s): 68.47.Fg, 71.18.+y, 79.60.-i, 68.37.Ef

Metals adsorbed on semiconductor surfaces form surface superstructures, which result from the reconstructions in the topmost layers of the substrates.¹ These systems have been extensively studied because they are intrinsically excellent platforms for low-dimensional physics such as phase transitions.^{2,3} Since the electrons in these systems are almost confined in a single monolayer thickness, they approach an ideal two-dimensional (2D) limit. Furthermore, since the surfaces are exposed to vacuum, the atomic positions and electronic structures can be directly probed with various techniques such as scanning tunneling microscopy (STM) and photoemission spectroscopy.

Among these metal-induced surface superstructures, Pb-overlayer phases on group-IV semiconductor (111) surfaces have been intensively studied because of their exotic properties. Some examples are the dilute $\sqrt{3}\times\sqrt{3}$ phases, which are formed with 1/3 ML (monolayer) of Pb adsorption on Si and Ge(111). These surfaces transform into 3×3 phases, which have a clear charge ordering at low temperature (LT).^{4,5} The driving force of the phase transitions has been intensively debated from the viewpoints of electron-phonon coupling, atomic dynamics, and electron correlation.⁶⁻⁸ Other examples are the so-called dense Pb overlayers on Si and Ge(111). A number of dense Pb overlayers are known around 1 ML of Pb coverage.^{9,10} The structures of these dense phases have been debated for a long time. The dense phases can easily have complex domain-wall structures depending on the initial Pb coverage in a very narrow region and the annealing history after deposition. Basically, the driving force for the formation of such domain-wall structures arises from the competition between adatom-adatom and adatom-substrate interactions, and their formation can be explained by the domain-wall theory in 2D.¹¹ However, the complexity has made it difficult to determine the coverage, atomic structure, and even the phase diagram of the dense Pb phases.^{10,12,13}

In the present study, we investigate the simplest Pb-induced dense phase on Ge(111), the so-called Pb/Ge(111)- $\beta\sqrt{3}\times\sqrt{3}$. This phase is the domain-wall-free limit of the above mentioned dense phases and generally considered to be a 4/3 ML Pb overlayer, which is shown in Fig. 1(b).^{9,14,15} The structure is characterized by 1 ML of Pb,

which saturates the T_1 sites of the substrate and the additional 1/3 ML of Pb on the H_3 sites. However, some indications of a lower saturation coverage at 1 ML have been given from Auger electron spectroscopy and STM, which lead to the Pb-trimer model in Fig. 1(a).¹⁶

In addition to the structural issues, this surface attracts interest because of its possible phase transition.¹⁷ A first-principles molecular dynamics study supported the 4/3 ML model for Pb/Ge(111)- $\beta\sqrt{3}\times\sqrt{3}$. The theory, furthermore, predicted a phase transition of the surface into a lower symmetry phase at LT.¹⁷ Figure 1(c) shows the theoretically calculated ground state, which loses the C_{3v} symmetry and is characterized by a chain structure with $3a_0$ periodicity along the $[10\bar{1}]$ direction (a_0 : lattice constant of the 1×1 unit). This phase transition was predicted as a kind of charge-density-wave (CDW) transition.

However, our STM image shown in this Brief Report clearly rules out the formation of the predicted CDW; the surface keeps the $\sqrt{3}\times\sqrt{3}$ structure in the C_{3v} symmetry even at 6 K. The discrepancy from the theory is understood from the electronic structure of the system. Our angle-resolved photoemission spectroscopy (ARPES) reveals a metallic band, which forms a well-nested hexagonal Fermi surface (FS). However, the nesting vector of the FS is far different from what is needed for the theoretically predicted CDW.¹⁷ Also, the simple estimation of the electron filling into the metallic band contradicts the generally believed 4/3 ML model but matches with the 1 ML model. The predicted CDW does not grow because the surface is described with the 1 ML model. The nested FS also does not yield a CDW

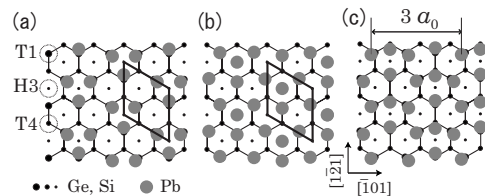


FIG. 1. (a) 1 ML and (b) 4/3 ML models for the Pb/Ge(111)- $\beta\sqrt{3}\times\sqrt{3}$ phase. The $\sqrt{3}\times\sqrt{3}$ unit cells are shown as lozenges. (c) The ground state theoretically predicted for the 4/3 ML model.

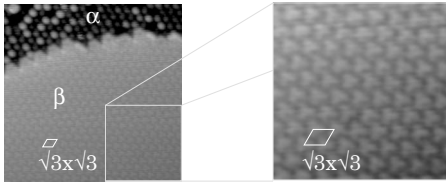


FIG. 2. A filled-state STM image ($140 \times 140 \text{ \AA}^2$) of the Pb/Ge(111)- $\beta\text{-}\sqrt{3} \times \sqrt{3}$ surface taken at 6 K. The tip voltage and tunneling current are 1 V and 0.3 nA, respectively. The α phase is seen in the upper part. The area enclosed with the square is enlarged in the right panel.

probably because of a negligible energy gain by electron-phonon coupling.

The experiments were performed in a commercial LT-STM system¹⁸ and in a VG-ADES 400 system with a He light source (He I α : $h\nu=21.22 \text{ eV}$). In the latter equipment, while the analyzer was rotated to collect energy distribution curves (EDCs), the sample was rotated with PC-controlled stepping motors to map the photoelectron intensity contours. A Ge(111) wafer (n type, $\rho < 15 \text{ \Omega cm}$) was cleaned in ultrahigh vacuum by several cycles of Ar⁺ sputtering (1 kV, 30 min) and annealing at 1123 K until a sharp $c(2 \times 8)$ reflection-high-energy electron diffraction (RHEED) pattern was obtained. The Pb/Ge(111)- $\beta\text{-}\sqrt{3} \times \sqrt{3}$ surface was prepared by depositing $\geq 4/3$ ML of Pb onto a clean Ge(111) surface at room temperature (RT) followed by annealing at 473 K. A sharp $\sqrt{3} \times \sqrt{3}$ pattern was observed by RHEED. In the STM chamber, the sample was prepared in the same way, then transferred *in vacuo* to a cold STM stage, and cooled down to 6 K at observation. During the experiment, the pressure was kept at $\leq 10^{-10}$ Torr.

Figure 2 shows a STM image, taken at 6 K, of the Pb/Ge(111)- $\beta\text{-}\sqrt{3} \times \sqrt{3}$ phase coexisting with the dilute $\sqrt{3} \times \sqrt{3}$, the so-called α phase. As seen through a comparison to the adjacent α phase, one finds that the $\beta\text{-}\sqrt{3} \times \sqrt{3}$ phase keeps the $\sqrt{3} \times \sqrt{3}$ periodicity even at 6 K. The enlarged image (the right panel of Fig. 2) shows a triangular structure with the C_{3v} symmetry in each $\sqrt{3} \times \sqrt{3}$ unit cell, which is the same as the previous STM image taken at 446 K.¹⁶ Thus, the $\sqrt{3} \times \sqrt{3}$ structure undergoes no phase transition down to 6 K.¹⁷

The above STM result contradicts the theory that predicts a CDW ground state on the surface.¹⁷ In order to know the possibility of the predicted CDW below 6 K, the nesting of the FS was investigated by mapping a photoelectron intensity contour at the Fermi energy (E_F), i.e., a FS map at RT [Fig. 3(a)]. The solid and broken lines in Fig. 3 indicate the $\sqrt{3} \times \sqrt{3}$ and 1×1 surface Brillouin zones (SBZs), respectively. A strong photoelectron intensity was obtained just outside of the first $\sqrt{3} \times \sqrt{3}$ -SBZ, which makes the features parallel to the six sides of the zone boundary. The photoelectron intensity loses its intensity in the other areas of the reciprocal space, but weak features are seen inside the hexagons of the $\sqrt{3} \times \sqrt{3}$ -SBZs. The weak traces should be parallel to the hexagons because the six strong features are parallel to the sides of the first $\sqrt{3} \times \sqrt{3}$ -SBZ and the contour should reflect the C_{3v} symmetry of the structure. A schematic of the obtained intensity contour is illustrated in Fig. 3(b). The FS of

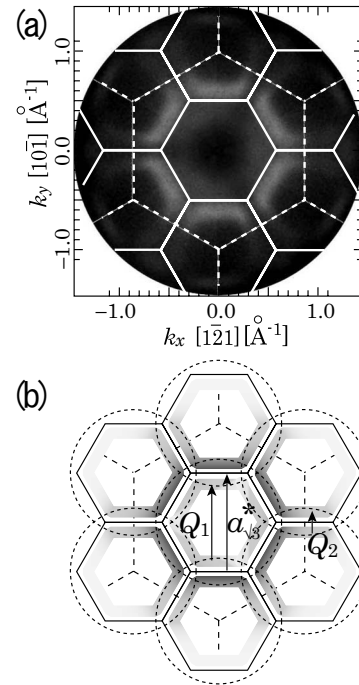


FIG. 3. (a) Photoelectron intensity map at E_F of the Pb/Ge(111)- $\beta\text{-}\sqrt{3} \times \sqrt{3}$ surface taken at RT. The solid (dotted) line indicates the $\sqrt{3} \times \sqrt{3}$ (1×1) SBZ. (b) Schematic of the intensity map. The hexagonal FSs are constructed by nearly-free-electron bands, which are drawn as dotted circles.

this system is perfectly hexagonal and meets a good nesting condition along the $[1\bar{1}0]$ and the other two equivalent directions.

In Fig. 3(b), the nesting vectors are drawn as arrows labeled $\mathbf{Q}_1 (=0.7\mathbf{a}_{\sqrt{3}}^*)$, where $\mathbf{a}_{\sqrt{3}}^*$ is the $\sqrt{3} \times \sqrt{3}$ reciprocal lattice vector) and $\mathbf{Q}_2 (=0.3\mathbf{a}_{\sqrt{3}}^*)$ if the nesting between neighboring SBZs is considered. The possible Peierls distortion by this FS would be the single- Q CDW with $\frac{2\pi}{Q_1}=1.2a_{\sqrt{3}}$ or $\frac{2\pi}{Q_2}=2.9a_{\sqrt{3}}$ periodicity in the $[10\bar{1}]$ and in the other two equivalent directions or the triple- Q CDW with $1.4a_{\sqrt{3}} \times 1.4a_{\sqrt{3}}$ or $3.3a_{\sqrt{3}} \times 3.3a_{\sqrt{3}}$ periodicity, where $a_{\sqrt{3}} = \sqrt{3}a_0$ ($1.2 \times \frac{2}{3} \approx 1.4$ and $2.9 \times \frac{2}{3} \approx 3.3$).¹⁹ However, none of them matches with the theoretically predicted periodicity of $3a_0$, and the predicted CDW is not likely.

The electronic structure was further investigated by measuring the band dispersion. Figure 4 shows a collection of EDCs taken at RT along the $[1\bar{2}1]$ direction in Fig. 4(a) and its grayscale image in Fig. 4(b). The EDCs were measured along the bold line in Fig. 4(c). Peak positions are marked with open circles in Fig. 4(a) and traced with thick lines. Four bands are seen within the binding energy (BE) of 1 eV from E_F [S_1 , S'_1 , S_2 , and S_3]. The S_1 band has its bottom around $\theta_e=26^\circ$ (\bar{M} point) and goes close to E_F with decreasing θ_e , and finally crosses E_F around $\theta_e=12^\circ$. Since this θ_e corresponds to the Fermi wave number of $k_F \sim 0.4 \text{ \AA}^{-1}$, the hexagonal FS observed in the first $\sqrt{3} \times \sqrt{3}$ -SBZ in Fig. 3(a) should be derived from this band.

The S_2 band is apparently insulating and has almost no dispersion at BE $\sim 1.0 \text{ eV}$. The S_3 state is also insulating and

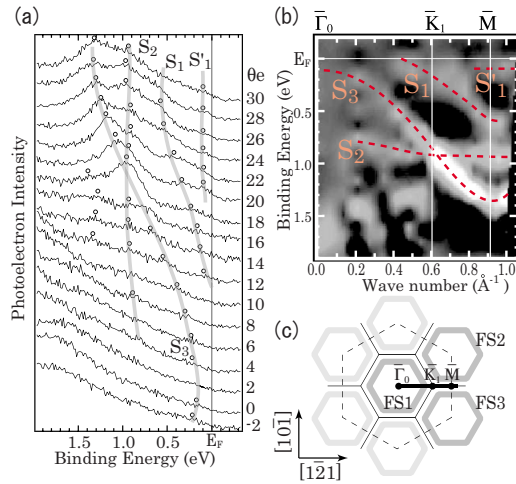


FIG. 4. (Color online) (a) A collection of EDCs of Pb/Ge(111)- $\beta\sqrt{3}\times\sqrt{3}$ along $[1\bar{2}1]$ taken at RT. The peak positions are marked with circles. θ_e is the emission angle measured from the surface-normal direction. (b) A grayscale image of the band dispersion obtained from the second derivatives of the obtained EDCs. (c) An illustration of SBZs and FS. The measurement was performed along the thick line in (c).

has its maximum and minimum at the $\bar{\Gamma}_0$ and \bar{M} points, respectively. Although the dispersion is similar to that of the bulk Ge band, it should be a surface state because the band maximum position at BE ~ 0.2 eV is too shallow for the bulk band.^{20,21} Finally, the S'_1 state makes a nondispersive feature at $\theta_e \geq 20^\circ$, which corresponds to the right side of the \bar{K}_1 point in Fig. 4(c). This band is interpreted in a nearly-free-electron model as a part of an intersection line of two adjacent free-electron parabolas, as discussed below. The obtained electronic structure, especially the metallicity, is largely different from a previous report on the same surface²² but rather close to that of the counterpart on Si(111).^{23,24}

The metallic band (S_1) is a hole pocket around $\bar{\Gamma}_0$. Recent photoemission studies showed a universal property in the band structures of group-III or group-IV metal-induced dense phases on Si(111), that is, the metallic bands should be basically nearly-free-electron-like with various electron fillings.^{24,25} Assuming also this universal property for Pb/Ge(111)- $\beta\sqrt{3}\times\sqrt{3}$, it is likely that the $\bar{\Gamma}_0$ -hole pocket is composed with large $\bar{\Gamma}_1$ -electron pockets centered at the neighboring SBZ. As shown by the dotted circles in Fig. 3(b), their radii are $r_{\text{free}} \approx 0.7 \text{ \AA}^{-1}$, which is larger than the $\sqrt{3}\times\sqrt{3}$ -SBZ.

We have performed a simple band calculation based on this nearly-free-electron model with a plane wave potential of $V(\mathbf{r}) = \sum_{\mathbf{G}} V_{\mathbf{G}} \exp(i\mathbf{G}\mathbf{r})$, where \mathbf{G} represents the reciprocal vector for the $\sqrt{3}\times\sqrt{3}$ lattice. An example of the calculated results is shown in Fig. 5, where the FS and the band dispersion along the bold line $[\bar{\Gamma}_0\text{-}\bar{K}_1\text{-}\bar{M}\text{-}\bar{K}_2]$ are shown in Figs. 5(a) and 5(b), respectively. The hexagonal FS and the two bands, S_1 and S'_1 , are clearly reproduced. The S_1 and S'_1 are derived from the same band in the different SBZs. They show dispersive (S_1) and nondispersive (S'_1) features between \bar{K}_1 and \bar{K}_2 and degenerate at both edges. The lower branch

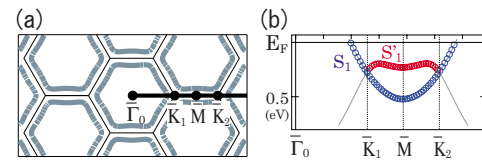


FIG. 5. (Color online) (a) FS and (b) band dispersion along the bold line in (a) of Pb/Ge(111)- $\beta\sqrt{3}\times\sqrt{3}$, which is simulated by using a nearly-free-electron model. The potentials in the periodicity of the shortest, the second shortest, and the third shortest G vectors of the $\sqrt{3}\times\sqrt{3}$ reciprocal lattice space were taken into account, all of which were simply set to be 0.5 eV. The $\sqrt{3}\times\sqrt{3}$ -SBZ is drawn with solid lines in (a).

between $\bar{\Gamma}_0$ and \bar{K}_1 , which is not traced with circles in Fig. 5(b), was not detected by photoemission probably because the photoemission structure factor is drastically changed at the zone boundary [\bar{K}_1 point] or it is hidden by the S_3 band in this region.

Considering the area ratio between the dotted circle and the $\sqrt{3}\times\sqrt{3}$ -SBZ in Fig. 3(b), the electron filling of this free-electron-like band is $2 \times \frac{\pi r_{\text{free}}^2}{\sqrt{3}(a_{\sqrt{3}})^2/2} = 2.9 \pm 0.4 \approx 3$ electrons per $\sqrt{3}\times\sqrt{3}$ unit cell. Let us compare this electron filling to that of a similar dense Pb/Si(111) phase. On Si(111), the perfect dense $\sqrt{3}\times\sqrt{3}$ is rarely formed with Pb and the so-called devil's staircase phases systematically develop in a very narrow region of the Pb coverage.²⁶ The devil's staircase phases are constructed by the linear combination of two basic building blocks of the dense $\sqrt{3}\times\sqrt{3}$ and $\sqrt{7}\times\sqrt{3}$ units. The structure of the dense $\sqrt{3}\times\sqrt{3}$ on Si(111) is described with the 4/3 ML model shown in Fig. 1(b), and the $\sqrt{7}\times\sqrt{3}$ has a Pb coverage lower than 1.2 ML.^{10,27} A recent ARPES study on such devil's staircase phases showed an increase in the electron filling of the free-electron-like band with the mixing ratio of the dense $\sqrt{3}\times\sqrt{3}$, which finally approached close to 13 electrons per $\sqrt{3}\times\sqrt{3}$ unit cell.²⁴ This is natural for the 4/3 ML model; the Pb atoms (four per $\sqrt{3}\times\sqrt{3}$ unit cell) release all the valence electrons (four per atom) to the free-electron band except those used in the covalent bonds with the unpaired electrons of underlying Si (three per $\sqrt{3}\times\sqrt{3}$ unit cell) ($4 \times 4 - 3 = 13$). However, our result of the electron filling (three electrons per $\sqrt{3}\times\sqrt{3}$ unit cell on Pb/Ge- $\beta\sqrt{3}\times\sqrt{3}$) cannot be compatible with the 4/3 ML model. Instead, the three-electron filling is possible if we consider the trimer model in Fig. 1(a) by taking into account covalent bonds not only between Pb and Si but also within the Pb trimers. Since the 1 ML model has three Pb atoms per $\sqrt{3}\times\sqrt{3}$ unit cell, the number of the valence electrons is 12 per $\sqrt{3}\times\sqrt{3}$ unit cell. Three of them would be used to make covalent bonds with the underlying Ge. In addition, it would be likely that six electrons per unit cell are used in the bonds among three Pb atoms. Thus, three electrons per $\sqrt{3}\times\sqrt{3}$ unit cell are left free in the trimer model ($3 \times 4 - 3 - 6 = 3$), which is consistent with our experimentally obtained band filling of Pb/Ge(111)- $\beta\sqrt{3}\times\sqrt{3}$. Note that this electron filling cannot be achieved with the 4/3 ML model even if Pb-Pb covalent bonds are taken into account; $7(=16-3-6)$ or $1(=16-3-6 \times 2)$ is possible but 3 is not.²⁸ Thus, the surface is likely described with the 1 ML trimer model, instead of the gener-

ally believed 4/3 ML model. The theoretically predicted CDW should not be yielded because it is based on the 4/3 ML model.

Note that the well-nested FS in Fig. 3 also does not yield a CDW at 6 K. The lack of a lock-in energy between the expected CDW and lattice would be the key to understand the absence of this CDW transition. The CDWs expected for \mathbf{Q}_1 and \mathbf{Q}_2 are largely incommensurate with the underlying lattice or have a wavelength that is more than five times larger than a_0 . A lock-in energy with the lattice cannot be gained when the nesting vector is largely incommensurate. It also becomes small as the wavelength of the CDW is large enough compared to the lattice constant of the underlying substrate.²⁹ In fact, there is no incommensurate CDW reported so far on surface systems. Also, there is no CDW on the Si or Ge surface whose wavelength is longer than $3a_0$.³⁰

In summary, the ground state and electronic structure of

the Pb/Ge(111)- $\beta\sqrt{3}\times\sqrt{3}$ surface have been investigated. In spite of the theoretical prediction,¹⁷ the surface undergoes no CDW transition down to 6 K. The nesting vectors in the FS do not match with the theory, and the simple estimation of the electron filling is not consistent with what is expected for the generally believed structure model of the surface on which the theory is also based. The surface should be described with the 1 ML trimer model instead of the 4/3 ML model. The absence of the nested-FS-driven CDW is thought to be for lack of enough energy gain by CDW lock in with the lattice.

Hideki Ohe is gratefully acknowledged for his help during the experiment. We also thank H. W. Yeom at Yonsei University for his useful discussion. This work was supported by Grants-In-Aid and A3 Foresight Program from the Japanese Society for the Promotion of Science and KOSEF.

*Present address: Institute of Physics and Applied Physics, Yonsei University, 134 Shinchon, Seoul 120-749, Korea.

¹V. G. Lifshits, A. A. Saranin, and A. V. Zotov, *Surface Phases on Silicon: Preparation, Structures, and Properties* (Wiley, Chichester, 1994).

²E. Bauer, in *Structure and Dynamics on Surfaces 2*, edited by W. Schommers and P. von Blanckenhagen (Springer, Berlin, 1987), pp. 115–180.

³S. Hasegawa, Y. Nagai, T. Oonishi, N. Kobayashi, T. Miyake, S. Murakami, Y. Ishii, D. Hanawa, and S. Ino, *Phase Transitions* **53**, 87 (1995).

⁴J. M. Carpinelli, H. H. Weitering, E. W. Plummer, and R. Stumpf, *Nature (London)* **381**, 398 (1996).

⁵O. Custance, J. M. Gómez-Rodríguez, A. M. Baró, L. Juré, P. Mallet, and J. -Y. Veullen, *Surf. Sci.* **482–485**, 1399 (2001).

⁶A. Mascaraque, J. Avila, E. G. Michel, and M. C. Asensio, *Phys. Rev. B* **57**, 14758 (1998).

⁷R. Cortés, A. Tejada, J. Lobo, C. Didiot, B. Kierren, D. Malterre, E. G. Michel, and A. Mascaraque, *Phys. Rev. Lett.* **96**, 126103 (2006).

⁸G. Profeta and E. Tosatti, *Phys. Rev. Lett.* **98**, 086401 (2007).

⁹L. Seehofer, G. Falkenberg, D. Daboul, and R. L. Johnson, *Phys. Rev. B* **51**, 13503 (1995).

¹⁰S. Stepanovsky, M. Yakes, V. Yeh, M. Hupalo, and M. C. Tringides, *Surf. Sci.* **600**, 1417 (2006).

¹¹P. Bak, *Rep. Prog. Phys.* **45**, 587 (1982).

¹²A. Petkova, J. Wollschläger, H. -L. Günter, and M. Henzler, *Surf. Sci.* **471**, 11 (2001).

¹³M. Hupalo, T. L. Chan, C. Z. Wang, K. M. Ho, and M. C. Tringides, *Phys. Rev. B* **66**, 161410(R) (2002).

¹⁴H. Huang, C. M. Wei, H. Li, B. P. Tonner, and S. Y. Tong, *Phys. Rev. Lett.* **62**, 559 (1989).

¹⁵R. Feidenhans'l, J. S. Pedersen, M. Nielsen, F. Grey, and R. L.

Johnson, *Surf. Sci.* **178**, 927 (1986).

¹⁶I. S. Hwang and J. A. Golovchenko, *Phys. Rev. Lett.* **71**, 255 (1993).

¹⁷F. Ancilotto, A. Selloni, and R. Car, *Phys. Rev. Lett.* **71**, 3685 (1993).

¹⁸N. Sato, T. Nagao, S. Takeda, and S. Hasegawa, *Phys. Rev. B* **59**, 2035 (1999).

¹⁹J. A. Wilson, F. J. DiSalvo, and S. Mahajan, *Adv. Phys.* **24**, 117 (1975).

²⁰R. D. Bringans, R. I. G. Uhrberg, and R. Z. Bachrach, *Phys. Rev. B* **34**, 2373 (1986).

²¹J. A. Carlisle, T. Miller, and T. C. Chiang, *Phys. Rev. B* **47**, 3790 (1993).

²²B. P. Tonner, H. Li, M. J. Robrecht, M. Onellion, and J. L. Erskine, *Phys. Rev. B* **36**, 989 (1987).

²³H. H. Weitering, A. R. H. F. Ettema, and T. Hibma, *Phys. Rev. B* **45**, 9126 (1992).

²⁴W. H. Choi, H. Koh, E. Rotenberg, and H. W. Yeom, *Phys. Rev. B* **75**, 075329 (2007).

²⁵E. Rotenberg, H. Koh, K. Rossnagel, H. W. Yeom, J. Schafer, B. Krenzer, M. P. Rocha, and S. D. Kevan, *Phys. Rev. Lett.* **91**, 246404 (2003).

²⁶M. Hupalo, J. Schmalian, and M. C. Tringides, *Phys. Rev. Lett.* **90**, 216106 (2003).

²⁷I.-S. Hwang, S. H. Chang, C. K. Fang, L. J. Chen, and T. T. Tsong, *Phys. Rev. Lett.* **93**, 106101 (2004).

²⁸One Pb-Pb bond and the other two equivalent bonds use 6(=2×3) electrons per $\sqrt{3}\times\sqrt{3}$ unit cell due to the C_{3v} symmetry of the structure.

²⁹G. Grüner, *Density Waves in Solids*, 1st ed. (Addison-Wesley, Reading, MA, 1994).

³⁰J. R. Ahn, P. G. Kang, K. D. Ryang, and H. W. Yeom, *Phys. Rev. Lett.* **95**, 196402 (2005).